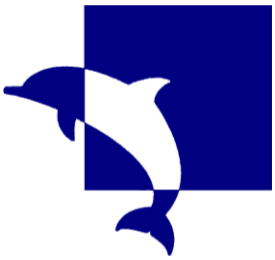

University
of Southampton

School of Engineering Sciences

Aerodynamics and Flight Mechanics

DNS Databases for Turbulent Couette and Poiseuille Flow

Z. W. Hu and N. D. Sandham

Technical Report: AFM-01/04

August 2001

UNIERSITY OF SOUTHAMPTON

SCHOOL OF ENGINEERING SCIENCES

AERODYNAMICS & FLIGHT MECHANICS RESEARCH GROUP

DNS Databases for Turbulent Couette and Poiseuille Flow

by

Z. W. Hu and N. D. Sandham

Report No. AFM-01/04

June 2001

DNS Databases for Turbulent Couette and Poiseuille Flow

Z. W. Hu and N. D. Sandham

Aerodynamics and Flight Mechanics Research Group
School of Engineering Sciences
University of Southampton, Southampton SO17 1BJ, U.K.
email: z.hu@soton.ac.uk n.sandham@soton.ac.uk

Abstract

Direct numerical simulations (DNS) of turbulent plane Couette and Poiseuille flow have been carried out at different Reynolds numbers in very large computational domains, which can ensure zero two-point correlations in both streamwise and spanwise directions. Good agreement with published results and balanced energy budgets have been achieved for the simulation results. DNS databases have been set up from Couette flow simulations up to $Re_w = 3400$ and Poiseuille flow up to $Re_\tau = 720$. Statistics of velocity, pressure and their gradients are collected, sufficient to evaluate all the terms in the transport equations for all second and third moments, as well as for turbulent dissipation. The databases can be used to validate and develop turbulence models for Reynolds averaged calculations and subgrid models for large-eddy simulations.

1 Introduction

Channel flow is a geometrically simple problem which has played an important role in understanding the mechanics of wall-bounded turbulent flow. Its simple geometry enables efficient direct numerical simulations (DNS) to be carried out.

DNS has been proved to be a very reliable tool for turbulence investigation and its ability to resolve details of turbulent flow has been utilized in many applications, for example validation of large-eddy simulation (LES) techniques, subgrid scale (SGS) models, and turbulence models used in Reynolds averaged Navier-Stokes (RANS) simulations. To valid the models, DNS databases can either be used directly to calculate each term in the transport equations to decide constants in the model, or indirectly by examination of the energy budgets. DNS databases of plane Poiseuille flow are now available up to some

This study is supported by EPSRC under Grant GR/M38865, and the Cray T3E time is provided by EPSRC Grant GR/M08424.

moderate Reynolds numbers (Moser, Kim & Mansour 1999). Rapidly increasing supercomputer power makes higher Reynolds number simulations feasible. DNS databases of turbulent channel flow at higher Reynolds number are useful in an effort to eliminate or at least quantify low Reynolds number effects.

Plane Couette flow is different from Poiseuille flow in that the flow is shear stress driven instead of pressure gradient driven. Very long large-scale structures exist in the core region (channel central region), whereas no clear large structure is found in Poiseuille flow (Lee & Kim 1991; Komminaho, Lundbladh & Johansson 1996; Hu & Sandham 2001). This makes the simulation of Couette flow more expensive than Poiseuille flow as a much bigger box is needed to resolve the large structure. So far no database has been published for Couette flow.

It is very important in the simulation of turbulent channel flow, especially for applications to acoustics, to have a large enough computational box so that large turbulent structures are correctly predicted and the low wavenumber behaviour is well demonstrated. Otherwise the periodic boundary condition applied in the two homogeneous directions will make the large structures infinitively long, resulting errors in the statistics. Large computational domains are used for all the simulations in present study so that the largest structures are included, this is ensured by checking that two-point correlation functions drop to zero.

In this study, turbulent Couette flow is simulated up to Reynolds number $Re_w = 3400$ and Poiseuille flow up to $Re_\tau = 720$ in very large computational domains, which can include the largest structures in the flow. DNS databases are established for 193 different statistical quantities, including high order moments of velocities, pressure and their gradients, so that all the terms for the transport equation of second and third order moments and turbulent dissipation can be calculated.

2 DNS of incompressible plane channel flow

2.1 Governing equations and summary of numerical method

The governing equations of incompressible turbulent flow, the continuity and momentum equations, are non-dimensionalized with a reference length $L^*_{\rm ref}$ equal to the channel half width h^*, and a reference velocity $U^*_{\rm ref}$, which is chosen as the friction velocity u^*_τ for Poiseuille flow, and the wall velocity u^*_w for Couette flow (both the upper and the lower walls move, with velocity u^*_w and $-u^*_w$ respectively). The non-dimensional quantities are then defined as (superscript $*$ stands for dimensional quantities)

$$u_i = u^*_i/U^*_{\rm ref}, \quad x_i = x^*_i/h^*, \quad p = p^*/(\rho^* U^*_{\rm ref} U^*_{\rm ref}), \quad t = t^* U^*_{\rm ref}/h^*.$$

The non-dimensional continuity equation and the rotation form of the momentum equations can be written as

$$\frac{\partial u_j}{\partial x_j} = 0, \tag{1}$$

$$\frac{\partial u_i}{\partial t} = \epsilon_{ijk} u_j \omega_k + \delta_{1i}\Lambda - \frac{\partial \Pi}{\partial x_i} + \frac{1}{Re}\frac{\partial^2 u_i}{\partial x_j \partial x_j}, \tag{2}$$

where ω_i is the vorticity, $\omega_i = \epsilon_{ijk}\partial u_k/\partial x_j$; Reynolds number is $Re = U^*_{\rm ref} h^*/\nu^*$, equal to $Re_\tau = u^*_\tau h^*/\nu^*$ for Poiseuille flow, and $Re_w = U^*_w h^*/\nu^*$ for Couette flow; ν^* is the kinematic viscosity of the fluid; $\Pi = p + u_i u_i/2$ is the non-dimensional modified pressure; ϵ_{ijk} is the permutation tensor and Λ is the driving mean pressure gradient.

The coordinates used in this paper are x for the streamwise direction, y for the spanwise direction, and z for the wall-normal direction with the channel walls at $z = \pm 1$, and the corresponding velocity components are denoted as (u, v, w).

Numerical solution of equations (1, 2) follows the spectral method of Kleiser & Schumann (1980), with Fourier and Chebyshev methods used for spatial discretizations, replacing the Adams-Bashforth time advance of Kleiser & Schumann (1980) with a third-order Runge-Kutta method for the convective term and the Crank–Nicolson method for the pressure and viscous terms. An implicit treatment is employed to avoid extremely small time steps in the near wall region owing to Chebyshev discretization. For each Runge–Kutta sub-step the discretized equation can be written as

$$\begin{aligned}\frac{u_i^{n+1} - u_i^n}{\triangle t} = a(\epsilon_{ijk} u_j \omega_k)^n &+ b(\epsilon_{ijk} u_j \omega_k)^{n-1} + \delta_{1i}\Lambda - \frac{1}{2}\left[\left(\frac{\partial \Pi}{\partial x_i}\right)^{n+1} + \left(\frac{\partial \Pi}{\partial x_i}\right)^{n}\right] \\ &+ \frac{1}{2Re}\left[\left(\frac{\partial u_i}{\partial x_j \partial x_j}\right)^{n+1} + \left(\frac{\partial u_i}{\partial x_j \partial x_j}\right)^{n}\right],\end{aligned} \tag{3}$$

where a and b are the Runge–Kutta sub-step coefficients, their values can be found in Sandham & Howard (1998); $n-1$, n and $n+1$ refer to successive sub-steps.

Poiseuille flow is a pressure gradient driven flow. Taking the Reynolds average of the streamwise momentum equation, we get

$$\Lambda = \frac{\partial}{\partial z}(\overline{u'w'} - \overline{\tau}_{xz}). \tag{4}$$

Where $\overline{\tau}_{xz} = \nu(\partial \overline{w}/\partial x + \partial \overline{u}/\partial z)$ is the mean viscous shear stress. The non-dimensional mean pressure gradient $\Lambda = 1$, so total non-dimensional shear stress in plane Poiseuille flow is equal to y. Plane Couette flow is driven by the movement of the walls. There is no mean pressure gradient for Couette flow, and the total shear stress is a constant across the channel.

2.2 Spatial derivatives

Spectral methods are an accurate way of forming spatial derivatives, for wavenumbers below some upper limit set by the spatial resolution. Fourier spectral methods require periodic boundary conditions, while Chebyshev methods can be applied to non-periodic directions. In the present problem, Fourier discretization is used for the channel horizontal plane, and the Chebyshev tau method is used for the wall-normal direction.

In the horizontal plane, a two-dimensional Fourier transformation from real to wave space is accomplished by a streamwise real to complex Fourier transformation, followed by a complex to complex Fourier transformation in the spanwise direction. After the streamwise transformation, only the mean and positive Fourier modes need to be stored due to symmetry. A real quantity $q(x,y)$ is transformed to $\tilde{q}(k_x,k_y)$ in discrete Fourier space by the successive operations:

$$\tilde{q}(k_{x_l},y_j)=\frac{1}{N_x}\sum_{i=0}^{N_x-1}q(x_i,y_j),e^{-\mathrm{i}2\pi li/N_x} \tag{5}$$

$$\tilde{q}(k_{x_l},k_{y_m})=\frac{1}{N_z}\sum_{j=0}^{N_z-1}\tilde{q}(k_{x_l},y_j)e^{-\mathrm{i}2\pi mj/N_y}, \tag{6}$$

where $\mathrm{i}=\sqrt{-1}$; x_i,y_j are the streamwise and spanwise coordinates of grid points with a total number of N_x and N_y in the two directions (both even). Uniform grids are used, so

$$x_i=\frac{L_x i}{N_x}, \qquad (0\le i\le N_x); \tag{7}$$

$$y_j=\frac{L_y j}{N_y}, \qquad (0\le j\le N_y). \tag{8}$$

The spatial wavenumbers k_{x_l},k_{y_m} are given by

$$k_{x_l}=\frac{2\pi l}{L_x}, \qquad (-N_x/2\le l\le N_x/2); \tag{9}$$

$$k_{y_m}=\frac{2\pi m}{L_y}, \qquad (-N_y/2\le m\le N_y/2). \tag{10}$$

L_x and L_y are the non-dimensional computational box lengths in the streamwise and spanwise directions.

The two-dimensional backward transformation is done with a spanwise complex to complex transformation, followed by a streamwise complex to real transformation:

$$\tilde{q}(k_{x_l},y_j)=\sum_{m=-N_y/2}^{N_y/2}\tilde{q}(k_{x_l},k_{y_m})e^{\mathrm{i}2\pi mj/N_y}, \tag{11}$$

$$q(x_i,y_j)=\tilde{q}(0,y_j)+2\sum_{l=1}^{N_x/2}\tilde{q}(k_{x_l},y_j)e^{\mathrm{i}2\pi li/N_x}. \tag{12}$$

Chebyshev transformations are used for the wall-normal direction with the help of the Chebyshev polynomial $T_n(z_k)$ (Canuto *et al*, 1987):

$$\tilde{q}(k_{z_n})=\sum_{k=0}^{N_z-1}q(z_k)T_n(z_k), \tag{13}$$

$$q(z_k) = \sum_{n=0}^{N_z-1} \tilde{q}(k_{z_n}) T_n(z_k). \tag{14}$$

Here N_z is the number of wall-normal grid points, whose coordinates z_k are a non-uniform cosine profile

$$z_k = \cos\left(\frac{\pi k}{N_z - 1}\right), \quad 0 \le k \le N_z - 1. \tag{15}$$

The nonlinear convective terms are calculated by zero-padding the separate factors in wave space by 50% before transforming back to real space, where the nonlinear terms are calculated. This '3/2 rule' de-aliasing has been applied whenever nonlinear quantities are required. Note that the process generates additional wavenumber components in the wave space representation, but these are truncated.

2.3 Initial condition

The initial flow fields consist of an approximate mean turbulent flow with superimposed artificial disturbances. Statistical data are accumulated only after the initial influence has disappeared and the flow has statistically settled down. The convergence is checked by comparing the statistical data in successive time segments, making sure that they are consistent. All statistical data are averaged over the horizontal plane and time.

More details of the numerical method used can be found in Kleiser & Schumann (1980), Canuto *et al.* (1987) and Sandham & Howard (1998). The parallel implementation of Sandham & Howard (1998) is employed for all the simulations.

3 DNS and validation

3.1 Details of simulations

Simulations of turbulent Poiseuille and Couette flow have been carried out at different Reynolds numbers, details of each simulation are given in table 1.

Table 1: Configurations of simulations.

Flow Type	Re_τ/ Re_w	Cray T3E PE hours	box length $(L_x \times L_y \times L_z)$	grid points $(N_x \times N_y \times N_z)$	$\triangle y^+$ at $z^+ = 9$	N $(z^+ < 9)$
Poiseuille	720	95,000	$12 \times 6 \times 2$	$512 \times 512 \times 321$	1.14	18
Poiseuille	360	30,000	$12 \times 6 \times 2$	$256 \times 256 \times 161$	1.58	13
Poiseuille	180	13,000	$24 \times 12 \times 2$	$256 \times 256 \times 121$	1.52	13
Couette	3400	14,000	$48 \times 12 \times 2$	$512 \times 256 \times 121$	1.45	13
Couette	1300	26,000	$192 \times 24 \times 2$	$1024 \times 256 \times 81$	1.52	13

Figure 1 shows the mean velocity profiles in wall units for Poiseuille and Couette flow simulations at different Reynolds numbers.

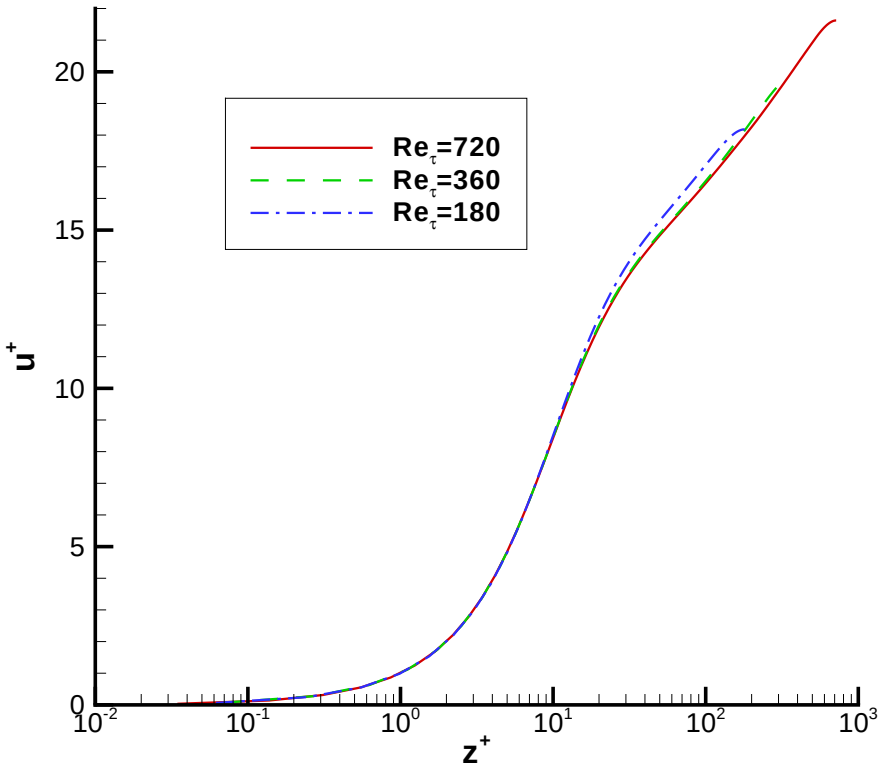

(a) Poiseuille flow

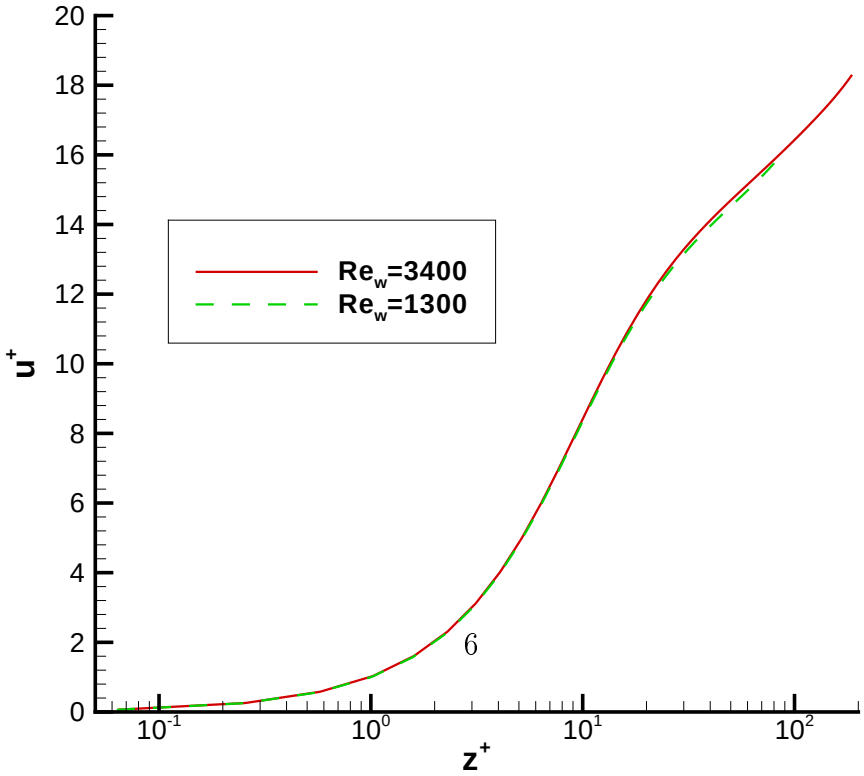

(b) Couette flow

Figure 1: Mean velocity profile in wall units.

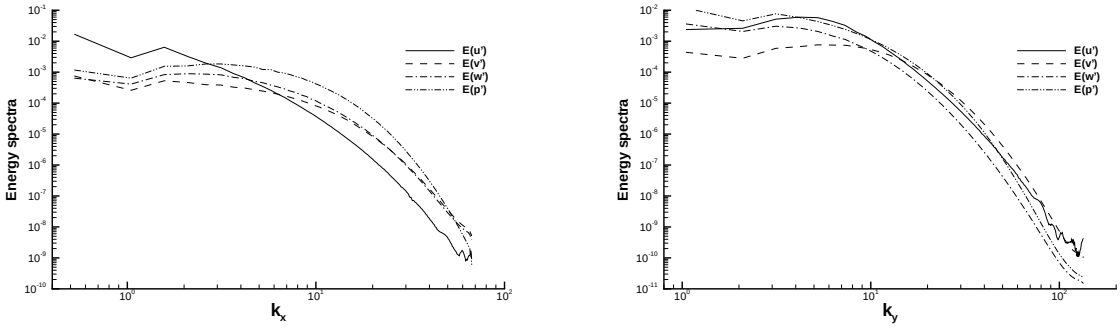

(a) Streamwise (b) Spanwise

Figure 2: Energy spectra of Poiseuille flow $Re_\tau = 360$ at $z^+ = 105.4$.

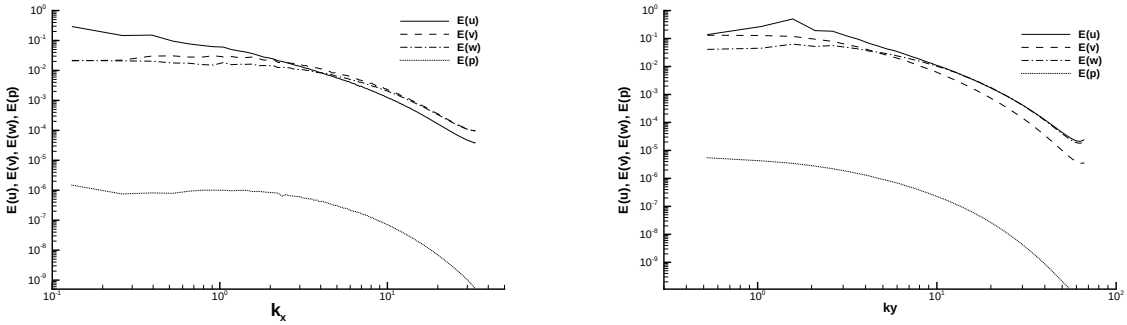

(a) Streamwise (b) Spanwise

Figure 3: Energy spectra of Couette flow $Re_w = 3400$ at centreline ($z^+ = 186.6$).

The same resolution in wall units is maintained for different Reynolds number simulations in the two periodic directions with $\Delta x^+ = 16.88$ and $\Delta y^+ = 8.44$ for Poiseuille flow and $\Delta x^+ = 15.38$ and $\Delta y^+ = 7.69$ for Couette flow. These are comparable with what was used in Kim, Moin & Moser (1987). In the wall-normal direction, at least 13 points are put in the near wall region ($z^+ < 9$), which has been proved to be sufficient for spectral methods. Energy spectra from simulations also give evidence for adequate spatial resolutions, as shown in figure 2 for Poiseuille flow at $Re_\tau = 360$ and figure 3 for Couette flow at $Re_w = 3400$.

3.2 Validation of DNS

3.2.1 Plane Poiseuille flow

A comparison of statistics with available DNS results and energy budgets of turbulent shear stresses has been performed to validate of DNS. Some typical results for Poiseuille flow with $Re_\tau = 360$ are given below.

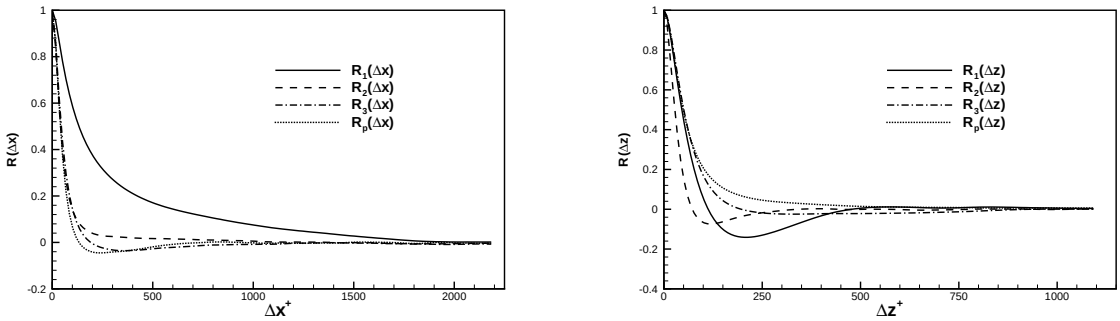

(a) Streamwise (b) Spanwise

Figure 4: Two-point correlations of velocity $R(u'), R(v')$, $R(w')$ and pressure $R(p')$ for Poiseuille flow $Re_\tau = 360$ at $z^+ = 105.4$.

In order to apply periodic boundary conditions to plane channel flow simulations, the computational domain must be large enough to include the largest turbulent structures. This can be checked after the simulation by examination of the zero two-point correlations. The two-point correlation functions of fluctuation velocity and pressure have been calculated.

$$R_i(\Delta x) = \frac{\overline{u_i'(x)u_i'(x+\triangle x)}}{\overline{u_i'^2}}, \qquad R_p(\Delta x) = \frac{\overline{p'(x)p'(x+\triangle x)}}{\overline{p'^2}}, \tag{16}$$

$$R_i(\Delta z) = \frac{\overline{u_i'(z)u_i'(z+\triangle z)}}{\overline{u_i'^2}}, \qquad R_p(\Delta z) = \frac{\overline{p'(z)p'(z+\triangle z)}}{\overline{p'^2}}. \tag{17}$$

Figure 4 shows the two-point correlations for Poiseuille flow at $y^+ = 105.4$. The two-point correlations fall to zero at maximum separation in both the streamwise and spanwise directions, demonstrating that present computational domain is adequate.

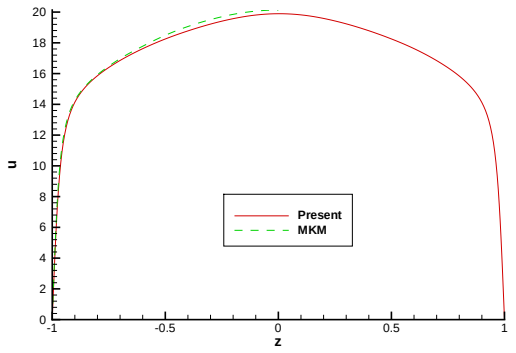

Figure 5: Mean velocity of Poiseuille flow compared with MKM.

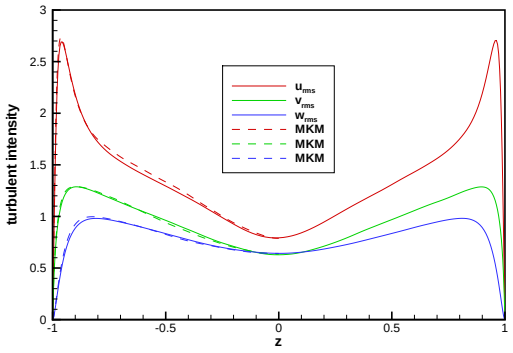

Figure 6: Turbulence intensities of Poiseuille flow compared with MKM.

The mean velocity and turbulent intensities shown in figures 5 and 6 are in good agreement with MKM ($Re_\tau = 395$). Symmetry of the results about the centreline indicates well converged statistics. The mean velocity profile collapses on the law of the wall $u^+ = (1/\kappa)\ln y^+ + B$ with $\kappa = 0.4$ and $B = 5.5$.

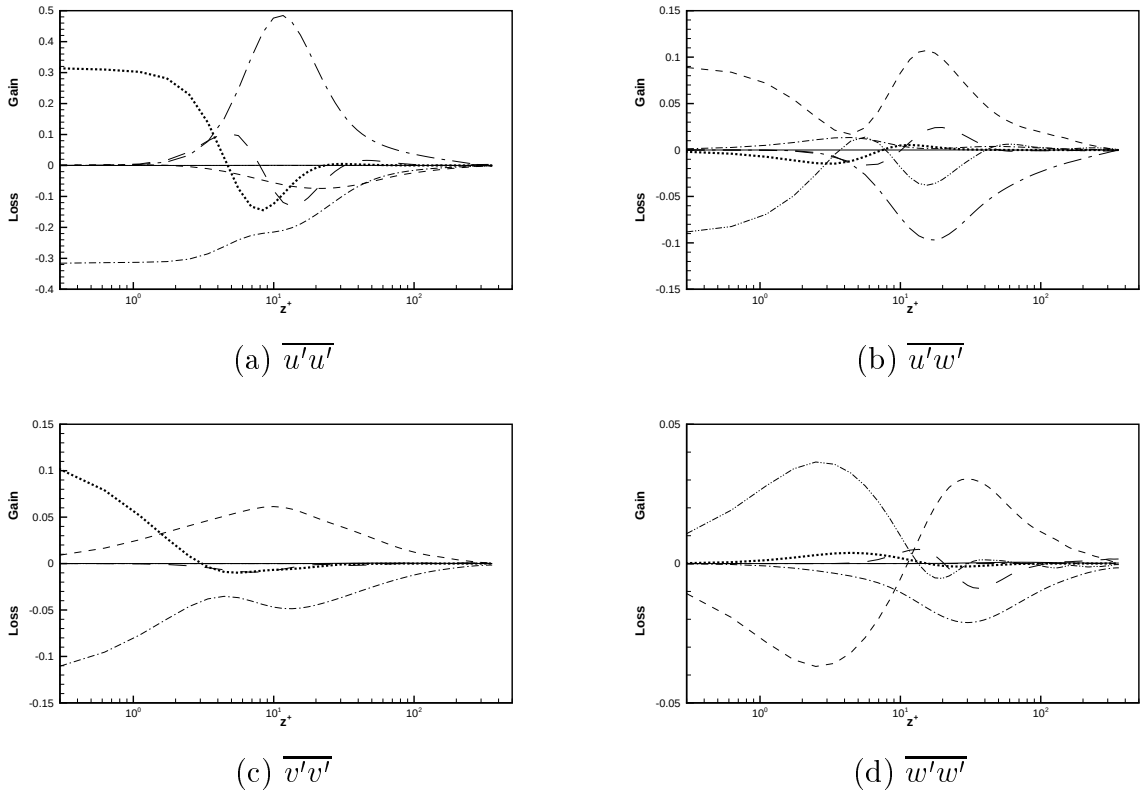

(a) $\overline{u'u'}$ (b) $\overline{u'w'}$

(c) $\overline{v'v'}$ (d) $\overline{w'w'}$

Figure 7: Energy budgets of Poiseuille flow Reynolds stresses. Solid line: P_{ij}, dash line: T_{ij}, dash-dotted line: D_{ij}, long dash line: $\partial J^u_{ijk}/\partial x_k$, dash-double-dotted line: $\partial J^p_{ijk}/\partial x_k$, dotted line: $\partial J^\nu_{ijk}/\partial x_k$)

The transport equations of Reynolds stresses, $R_{ij} = \overline{u_i' u_j'}$, can be derived from the continuity and momentum equations, as

$$\frac{\partial R_{ij}}{\partial t} + \overline{u}_k \frac{\partial R_{ij}}{\partial x_k} = P_{ij} + T_{ij} - D_{ij} - \frac{\partial}{\partial x_k}(J^u_{ijk} + J^p_{ijk} + J^\nu_{ijk}), \tag{18}$$

where terms on the right hand side are

$$\left.\begin{aligned} P_{ij} &= -\left(R_{ik}\frac{\partial \overline{u}_j}{\partial x_k} + R_{jk}\frac{\partial \overline{u}_i}{\partial x_k}\right) \\ T_{ij} &= \overline{p'\left(\frac{\partial u_i'}{\partial x_j} + \frac{\partial u_j'}{\partial x_i}\right)} \\ D_{ij} &= \frac{2}{Re}\overline{\frac{\partial u_i'}{\partial x_k}\frac{\partial u_j'}{\partial x_k}} \\ J^u_{ijk} &= \overline{u_i' u_j' u_k'} \\ J^p_{ijk} &= \overline{p' u_j'}\delta_{ik} + \overline{p' u_i'}\delta_{jk} \\ J^\nu_{ijk} &= -\frac{1}{Re}\frac{\partial R_{ij}}{\partial x_k} \end{aligned}\right\} \qquad (19)$$

In the above equations, P_{ij} is the production due to mean velocity gradients, T_{ij} is the pressure-strain term, D_{ij} is the 'dissipation' (it is different from the real dissipation term ε, which represents the transfer rate of energy from turbulence to heat) and J_{ijk} is the turbulence flux term, with J^u_{ijk} contribution from the turbulence transport term, J^p_{ijk}, the pressure transport term and J^ν_{ijk}, the viscous transport term. After the flow has become statistically stable, the terms on the right hand side should sum to zero.

Plane Poiseuille and Couette flow are homogeneous in the streamwise and spanwise directions, and the Reynolds stresses R_{13} and R_{23} are zero. Budgets of the all remaining turbulent shear stresses have been calculated as a check on our simulation results, as shown in Figure 7. The budget balances (sum of all terms on the right hand side) are of the order of 10^{-4}. All quantities are normalized by u_τ^{*4}/ν^*.

3.2.2 Plane Couette flow

It is well known that very long structure exists in the core area of Couette flow; this makes Couette flow simulations more difficult as very large computational domains are needed to include this structure. Very few DNS of Couette flow are available at low Reynolds numbers, e.g. Komminaho *et al.* (1996) at $Re_w = 750$ and Kristoffersen, Bech & Andersson (1993) (referred to as KBA hereafter) at $Re_w = 1300$. In this section, DNS of results of Couette flow $Re_w = 1300$ are compared with KBA.

The computational box used in present study is large enough to allow periodic boundary conditions to be applied in both streamwise and spanwise directions, as demonstrated by the streamwise and spanwise two-point correlations shown in figure 8 at the channel centreline, where the worst situation for two-point correlations occurs.

Figure 9 show the mean velocity of Couette flow, which is in good agreement with KBA. Plane Couette flow is driven by the two walls moving in opposite directions, and has a typical S-shaped mean velocity profile, leading to a non-zero mean velocity gradient at the centreline. Its non-dimensional value is 0.1924 for $Re_w = 1300$ from the present

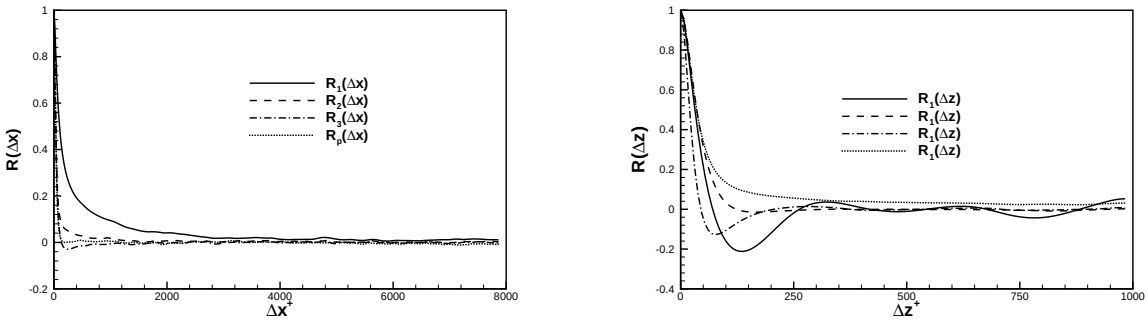

(a) Streamwise (b) Spanwise

Figure 8: Two-point velocity correlations of Couette flow at channel centreline.

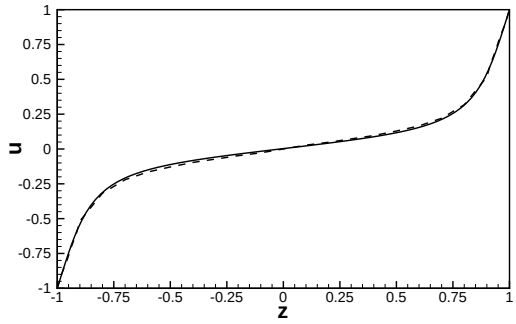

Figure 9: Mean velocity of Couette flow.

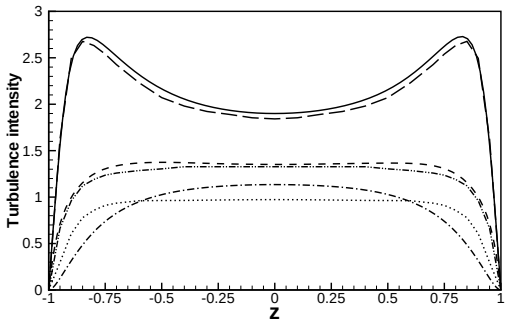

Figure 10: Turbulence intensities of Couette flow.

simulations. Another simulation at higher Reynolds number $Re_w = 3400$ gives 0.1980. Tillmark *et al.* (1993) collected available experimental data and found that the non-dimensional mean velocity gradient at the centreline varies between 0.15 and 0.3 for $Re_w = 750 \sim 19000$. DNS of Komminaho *et al.* (1996) for Reynolds number $Re_w = 750$ gave a value of 0.18. This mean velocity gradient gives Couette flow a finite shear stress at centreline, which leads to non-zero production as well as dissipation at the channel centreline (figure 11(a)).

Turbulence intensities for plane Couette flow are given in figure 10, with all quantities normalized by u_τ^*. Results of KBA are also plotted with thin lines for comparison. The streamwise and spanwise turbulence intensities of KBA are close to the present results in the near wall region but smaller elsewhere; the differences are almost certainly caused by the coarser resolution and smaller box used in KBA. KBA used a second-order central finite difference method for all spatial derivatives and a second-order Adams–Bashforth scheme for time advance. The grid spacing used by KBA is 11.12 and 8.34 wall units for the streamwise and spanwise directions respectively, compared to 15.38 and 7.69 for the present simulation. Although their streamwise grid spacing is smaller, the effective

resolution is still lower because of the higher accuracy of the present spectral method. The wall-normal resolution of KBA is also lower with only 64 points, compared with 81 points in the present simulation. Comparison between test cases with different resolutions shows that coarse resolution will give smaller turbulence intensities in the streamwise and spanwise directions. Another difference is that the computational box used in KBA is $4\pi h^* \times 2\pi h^* \times 2h^*$, which is not large enough to get two-point correlations dropping to zero, as shown in their two-point correlation results.

Large differences exist in the wall-normal turbulence intensity, with the results of KBA being flat in the channel centre region. Komminaho *et al.* (1996) ran a Couette flow simulation at $Re_w = 750$ in a box of $28\pi h^* \times 8\pi h^* \times 2h^*$, and their results for wall-normal turbulence intensity also show a parabolic profile with no flat region.

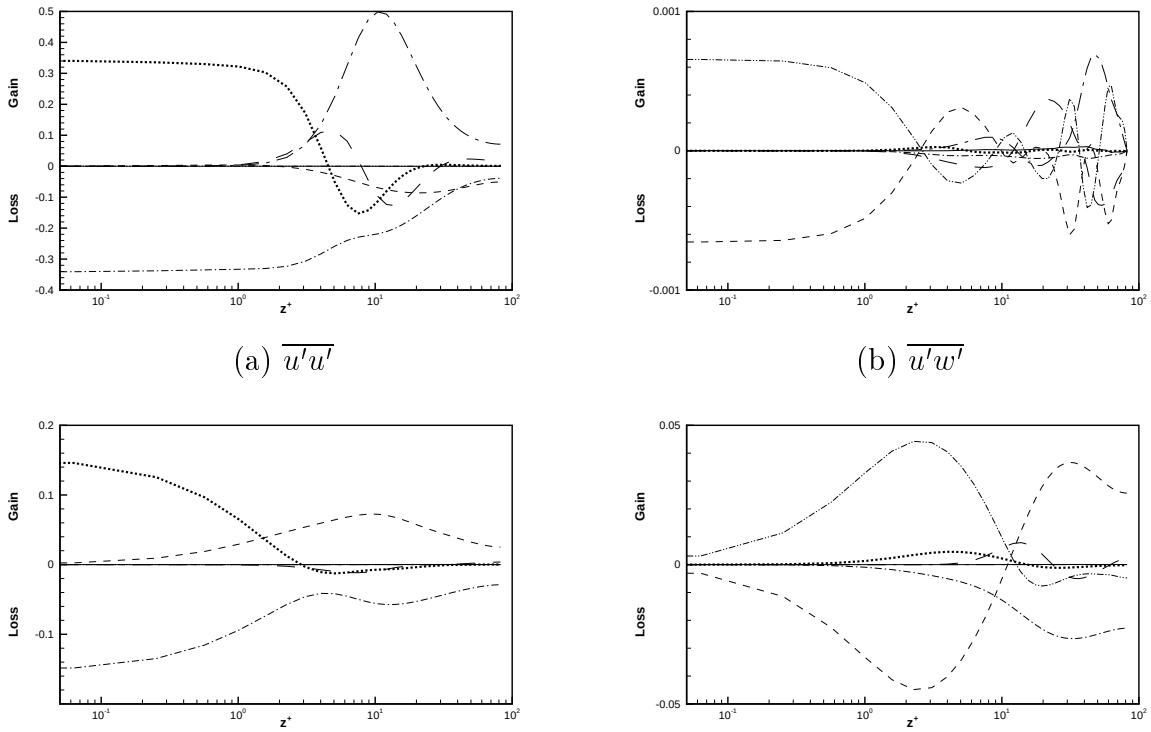

(a) $\overline{u'u'}$ (b) $\overline{u'w'}$

(c) $\overline{v'v'}$ (d) $\overline{w'w'}$

Figure 11: Energy budgets of Couette flow Reynolds stresses. Solid line: P_{ij}, dash line: T_{ij}, dash-dotted line: D_{ij}, long dash line: $\partial J^u_{ijk}/\partial x_k$, dash-double-dotted line: $\partial J^p_{ijk}/\partial x_k$, dotted line: $\partial J^\nu_{ijk}/\partial x_k$)

Budgets of Couette flow Reynolds stresses are shown in figure 11. All quantities are normalized by u_τ^{*4}/ν^*. Very good balances of energy have been achieved, demonstrating high accuracy of the simulation results. The maximum imbalance is less than 2×10^{-4}.

4 DNS databases

The following is a list of statistical moments collected from the simulation after the flow has statistically settled down. All the quantities have been averaged over the two periodic directions and time, which is denoted with angle brackets. Numbers in the brackets refer to the number of quantities collected for this term.

$< u_i >$ (3)	$< u_i u_j >$ (6)	$< u_i u_j u_k >$ (10)	$< u_i u_j u_k u_l >$ (15)
$< p >$ (1)	$< p^2 >$ (1)	$< p^3 >$ (1)	$< p^4 >$ (1)
$< p u_i >$ (3)	$< p u_i u_j >$ (6)	$< p \frac{\partial u_i}{\partial x_j} >$ (9)	$< \frac{\partial u_i}{\partial x_j} \frac{\partial u_m}{\partial x_n} >$ (45)
$< u_i \frac{\partial u_j}{\partial x_k} >$ (27)	$u_k < \frac{\partial u_i}{\partial x_m} \frac{\partial u_j}{\partial x_m} >$ (18)	$< \frac{\partial u_i}{\partial x_j} \frac{\partial u_i}{\partial x_k} \frac{\partial u_j}{\partial x_k} >$ (1)	$< \frac{\partial p}{\partial x_i} \frac{\partial u_j}{\partial x_k} >$ (27)
$< p > \frac{\partial u_i u_j}{\partial x_k}$ (18)	$\frac{\partial^2 u_i}{\partial x_j \partial x_k} \frac{\partial^2 u_i}{\partial x_j \partial x_k}$(1)		

One application of the data from DNS is to validate turbulence models, for use in engineering applications. A total of 193 statistics are collected in the database. All the terms of the transport equations of second and third moments and turbulent dissipation can be calculated from the above statistics. This database can then be used to to valid and develop new RANS and LES models.

The DNS databases are available at http://www.afm.ses.soton.ac.uk/∼zhi.

5 Summary

Direct numerical simulations of turbulent Couette and Poiseuille flow have been carried in very large computational domains, which can ensure zero two-point correlations in both streamwise and spanwise directions. The simulations of Couette flow were run up to Reynolds number $Re_w = 3400$ and Poiseuille flow up to $Re_\tau = 720$. 193 statistics were collected to establish the DNS databases, which enable the calculation of all the terms in the transport equations of second and third moments and turbulent dissipation. The databases can be used for validation of turbulence models and LES techniques and developing new turbulence models.

References

[1] C. Canuto, M. Y. Hussaini, A. Quarteroni, and T. A. Zang. *Spectral Methods in Fluid Dynamics*. Springer–Verlag, New York, 1987.

[2] Z. W. Hu and N. D. Sandham. Large-domain simulation of plane Couette and Poiseuille flow. In E. Lindborg *et al.*, editor, *Proceedings of Turbulence Shear Flow Pheomena, Second international symposium*, pages 377–382. KTH, Stockholm, June 27-29 2001.

[3] J. Komminaho, A. Lundbladh, and A. Johansson. Very large structures in plane turbulent Couette flow. *Journal of Fluid Mechanics*, 320:259–285, 1996.

[4] L. Kleiser and U. Schumann. Treatment of incompressibility and boundary layer conditions in 3D numerical spectral simulations of plane channel flows. In E. H. Hirschel, editor, *Proc. 3rd GAMM Conf. on Numerical Method in Fluid Mechanics*, pages 165–173. Vieweg, 1980.

[5] J. Kim, P. Moin, and R. Moser. Turbulence statistics in fully developed channel flow at low Reynolds number. *Journal of Fluid Mechanics*, 177:133–166, 1987.

[6] R. Kristoffersen, K. H. Bech, and H. I. Andersson. Numerical study of turbulent plane Couette flow at low Reynolds number. *Applied Scientific Research*, 51:337–343, 1993.

[7] M. J. Lee and J. Kim. The structure of turbulence in a simulated plane Couette flow. In *Proceedings of 8th Symposium on Turbulent Shear Flows*. Vieweg, Sept. 1991.

[8] R. D. Moser, J. Kim, and N. N. Mansour. Direct numerical simulation of turbulent channel flow up to Re_τ=590. *Physics of Fluids*, 11(4):943–945, 1999.

[9] N. D. Sandham and R. J. A. Howard. Direct simulation of turbulence using massively parallel computers. In D. R. Emerson et al., editors, *Parallel Comp. Fluid Dynamics*, pages 23–32. Elservier, 1998.

[10] N. Tillmark and P. H. Alfredsson. Turbulence in plane Couette flow. *Applied Scientific Research*, 51:237–241, 1993.